The Electronic Structure of Helicene–Bisquinone Anion Radicals

Charles A. Liberko,[†] Larry L. Miller,*[,†] Thomas J. Katz,*[,‡] and Longbin Liu[‡]

Contribution from the Department of Chemistry, University of Minnesota, Minneapolis, Minnesota 55455, and the Department of Chemistry, Columbia University, New York, New York 10027. *Received October 13, 1992*

Abstract: Helicene–bisquinones with five, six, seven, and eight rings were studied by cyclic voltammetry, and their anion radicals, prepared electrochemically, were studied by visible, near-IR, and ESR spectroscopy. The large separation between reduction potentials, the well-defined absorptions at very long wavelengths, and hyperfine splittings in the ESR spectra that are independent of temperature all imply that unlike linear analogs, the helical bisquinone anion radicals have delocalized electronic structures. PPP semiempirical calculations correctly account for these experimental observations. They do so, however, only if the assumption is made that the odd electron is not only delocalized between the conjugated rings but also across the gap separating the ends, as in a Möbius array.

Previous studies have revealed unusual electronic effects in radical anions of π-conjugated systems that have two or more electroactive groups.[1] One interesting observation concerns the difference between the anion radicals of different linear bisquinones. $\mathbf{8}^-$ shows a well-defined absorption in the near-IR, at 1335 nm, and an ESR spectrum that is independent of temperature. Ab initio calculations show that the near-IR band is a π^*–π^* transition and that the odd-electron in the radical anion should be delocalized.[1d] In contrast, $\mathbf{9}^-$ has a very broad, featureless absorption extending throughout the visible and near-IR regions. The ESR spectrum is temperature dependent, and ab initio calculations imply that the odd electron is localized on one or the other quinone moieties and jumps back and forth.[1c] Unlike $\mathbf{8}^-$, $\mathbf{9}^-$ has a double minimum on its potential energy surface.

Another interesting observation concerns the difference between the anion radicals of linear and helical bisquinones. In a recent report[2] communicating the synthesis, electrochemistry, near-IR absorptions, and preliminary ESR studies of anion radicals $\mathbf{1}^-$–$\mathbf{4}^-$, we showed that the odd electron in the helical quinone anion radicals are fully delocalized, whereas in the linear analogue of $\mathbf{1}^-$, it is localized. We suggested that the reason might be that the proximity of the helical array's extremities allows electrons to move easily between the ends and therefore cyclically throughout the array. In this paper we report an ESR study that is more complete and that, along with studies of near-IR spectra and electrochemical behavior, extends to structures **5**–**7**. We also report the results of semiempirical calculations supporting the idea that the π-electrons in these helical anion radicals delocalize as on a Möbius array.

Previous investigations of the [6]helicene hydrocarbon anion radical[3] did not unearth evidence of such delocalization, whereas investigations of neutral helicenes[4a,b] and the anion radicals of heterohelicenes,[4c] in which transannular delocalization was specifically sought, showed only that it was unimportant. Of particular interest in this regard is a photoelectron spectroscopic study[4a] of helicene hydrocarbons supplemented by extensive semiempirical molecular orbital calculations. It suggested that transannular overlap is repulsive and minimized by a rehybridization of the sp^2 carbon atoms.

Experimental Section

Cyclic voltammetry was performed at a glassy carbon electrode using dimethyl formamide 0.1 M in tetra-*n*-butylammonium tetrafluoroborate under an inert atmosphere. The SCE reference electrode was held in electrical contact via a layer of DMF agar and aqueous agar. Electrochemical reductions were performed in a divided cell with a carbon sponge cathode and a carbon rod anode. The solution containing 0.1 M tetra-*n*-butylammonium tetrafluoroborate and 1.0–0.1 mM diquinone was reduced at a potential 100 mV more negative than $E_{1/2}$ until the current had dropped to 0.1% of the initial flux. Typical reductions passed 0.9 equiv/mol.

Table I. Cyclic Voltammetric Potentials for Bisquinones[a]

quinone	$-E_1^0$, V	$-E_2^0$, V	$\Delta E^{0,b}$ mV
1	0.44	0.91	470
2	0.56	0.94	380
3	0.56	0.87	310
4	0.61	0.88	270
5	0.52	0.93	410
6	0.67	0.98	310
7	0.57	*c*	
8	0.42	0.92	500
9	0.72	0.84	120

[a] In DMF containing 0.1 M *n*-$Bu_4N^+BF_4^-$, compared to SCE. The values listed are the means of the anodic and cathodic peak potentials. [b] E_1^0–E_2^0. [c] Irreversible.

Vis and near-IR spectra were recorded on a Cary 17 spectrometer. ESR was carried out on a Brucker ESP 300. Simulations were performed with a program provided by Paul Kasai (IBM, Almaden Labs) and modified by Vince Cammarata. PPP type semiempirical calculations[5] were performed on a microcomputer using program QCMPO54 purchased from the Quantum Chemistry Program Exchange. The program was modified to accept molecules with more than 30 atoms and to allow for nonplanar geometries. Standard parameters[6] were used to calculate the electronic structures of the neutral molecules. The transannular overlap integrals were taken from Koutecky and Paldus.[7]

The synthesis of quinones **1**–**4** was reported previously,[2,8] and that of **5** and **6** will be reported separately. Quinone **7** was synthesized by Manning et al.'s modification[9] of the procedure of Rosen and Weber.[10]

[†] University of Minnesota.
[‡] Columbia University.

(1) (a) Rak, S. F.; Miller, L. L. *J. Am. Chem. Soc.* **1992**, *114*, 1388. (b) Rak, S. F. Jozefiak, T. H.; Miller, L. L. *J. Org. Chem.* **1990**, *55*, 4794. (c) Jozefiak, T. H.; Almlöf, J. E.; Feyereisen, M. W.; Miller, L. L. *J. Am. Chem. Soc.* **1989**, *111*, 4105. (d) Almlöf, J. E.; Feyereisen, M. W.; Jozefiak, T. H.; Miller, L. L. *J. Am. Chem. Soc.* **1990**, *112*, 1206. (e) Jozefiak, T. H.; Miller, L. L. *J. Am. Chem. Soc.* **1987**, *109*, 6560.

(2) Yang, B.; Liu, L.; Katz, T. J.; Liberko, C. A.; Miller, L. L. *J. Am. Chem. Soc.* **1991**, *113*, 8993 and references cited therein.

(3) (a) Fey, H. J.; Kurreck, H.; Lubitz, W. *Tetrahedron* **1979**, *35*, 905. (b) Allendoerfer, R. D.; Chang, R. *J. Magn. Reson.* **1971**, *5*, 273. (c) Weissman, S. I.; Chang, R. *J. Am. Chem. Soc.* **1972**, *94*, 8683.

(4) (a) Obenland, S.; Schmidt, W. *J. Am. Chem. Soc.* **1975**, *97*, 6633 and references cited therein. (b) Deb, B. M.; Kavu, G. *Can. J. Chem.* **1980**, *58*, 258. (c) Tanaka, H.; Ogashiwa, S.; Kawazuwa, H. *Chem. Lett.* **1981**, 585. (d) For general reviews of helicenes, see: Laarhoven, W. H.; Prinsen, W. J. C. *Top. Curr. Chem.* **1984**, *125*, 63–130. Meurer, K. P.; Vögtle, F. *Top. Curr. Chem.* **1985**, *127*, 1–76.

(5) Pariser, R.; Parr, R. G. *J. Chem. Phys.* **1953**, *21*, 466.

(6) Griffiths, J. *Dyes Pigm.* **1982**, *3*, 211.

(7) Koutecký, J.; Paldus, J. *Collection Czechoslov. Chem. Commun.* **1962**, *27*, 599.

(8) Liu, L.; Katz, T. J. *Tetrahedron Lett.* **1990**, 3983.

0002-7863/93/1515-2478$04.00/0

Table II. Calculated and Experimental Absorption Maxima for $\pi^*-\pi^*$ Transitions

anion	$-E_{SOMO}$, eV	$-E_{LUMO}$, eV	$\pi^*-\pi^*$ calc/eV	$\pi^*-\pi^*$ obs/eV (nm)
1^-	4.00	3.34	0.66	0.89 (1400)
2^-	3.85	3.30	0.55	0.68 (1825)
3^-	3.75	3.50	0.25	0.57 (2190)
4^-	3.71	3.50	0.21	0.56 (2210)
5^-	3.72	3.07	0.65	0.87 (1420)
6^-	3.40	2.97	0.44	0.62 (2000)

Results and Discussion

Cyclic Voltammetry. The bisquinones all show two reversible one-electron couples, each with a 60-mV separation between the anodic and cathodic peaks. Peak currents vary linearly with the concentration as well as with the square root of the sweep rate. Coulometry confirms that each couple is a one-electron process. Apparent $E°$s, the midpoints of the anodic and cathodic peaks, are listed in Table I.

$E°$ values can sometimes be used to distinguish localized and delocalized electronic structures. If, for example, the first reduction potential of the bisquinone were more positive than that of a suitable model like monoquinone **7**, it might be concluded that the added electron occupies an orbital extending over both quinones. Although the first reduction potential of **1** is slightly more positive than that of **7**, this is not true of the other helical bisquinones (**2**–**6**). Thus the reduction potentials alone do not show whether the unpaired electron in the helical bisquinone anion radicals are delocalized.

The separation between the two reduction potentials may also indicate the extent of delocalization, for it reflects electron repulsion within the dianion. Because the separation of reduction potentials in the five-ringed diquinone **9** is 120 mV,[1c] a similar value might be expected for the helical analogue **1**. In fact, however, as shown in Table I, the measured separation in **1** is 470 mV, similar to the separation in the reduction potentials of **8**.[1d] Since, as discussed above, the anion radical of **8** is known to be delocalized, while that of **9** is localized, the implication is that the anion radical of **1**, unlike that of **9** but like that of **8**, is delocalized. A similar conclusion can be reached for the six-ringed anion radical $\mathbf{2}^-$, which has a separation of reduction potentials of 380 mV. As the number of rings increases to seven and eight rings, the separation between the reduction waves becomes smaller, which can be explained by the larger size of either the localized or delocalized structures decreasing electron repulsions in the dianions. Thus for the larger bisquinones the peak separations are consistent with delocalized structures but do not clearly distinguish them from those that are localized.

Electronic Excitations. The near-IR absorption maxima for the helical bisquinone anion radicals are recorded in Table II. We indicate here reasons for assigning them to be $\pi^*-\pi^*$ transitions. $\mathbf{1}^-$, which shows a well-defined absorption maximum at 1400 nm ($\log \epsilon = 3.32$), is similar to the delocalized $\mathbf{8}^-$, which absorbs maximally at 1335 nm. The localized $\mathbf{9}^-$, on the other hand, has a very broad featureless absorption, which extends throughout the visible and near-IR region. For $\mathbf{1}^-$, as for $\mathbf{8}^-$, the solvent has only a small effect on the wavelength of maximum absorption: 1400 in DMF, 1350 in CH_2Cl_2, 1420 nm in methyltetrahydrofuran. This very small variation is consistent with a $\pi^*-\pi^*$ transition[1] and not with a charge-transfer transition.[11] Beer's law was obeyed for concentrations between 0.5 and 5.0 mM, the line extrapolating to the origin, indicating that the transitions are unimolecular. The band widths at half height are $\mathbf{1}^-$, 4900; $\mathbf{2}^-$, 4300; $\mathbf{3}^-$, 2400; and $\mathbf{4}^-$, 3700 cm^{-1}. These widths are in the approximate range expected for an intervalence transfer[11c,d] but could be due to the vibrational structure associated with a $\pi^*-\pi^*$ excitation.

In the series of helicene bisquinones, the transitions move to lower energy as the number of rings increases. In DMF, $\mathbf{3}^-$ absorbs maximally at 2190 nm ($\log \epsilon = 3.32$) and $\mathbf{4}^-$ absorbs at 2210 nm ($\log \epsilon = 3.32$). In CH_2Cl_2, $\mathbf{3}^-$ absorbs at 2050 nm. The trend in the transition energies and the similarity in the ϵ values suggests that all of these transitions are of the same type. The transitions are interesting because they appear at wavelengths that are extremely long for unimolecular electronic transitions. These wavelengths can, however, be calculated if the assumption is made that they are $\pi^*-\pi^*$ transitions.

PPP Calculations

We have previously shown that PPP calculations can be used to accurately calculate the reduction potentials, wavelengths of maximum absorption, and proton hyperfine splitting constants for quinone anion radicals.[12] Using the same method, we calculated the electronic structures of the helicene bisquinone anion radicals. For each of the anion radicals, initial results correlated poorly with the experimental transition energies. For example, the transition energy for $\mathbf{1}^-$ was computed to be 0.15 eV, not close to the experimental value of 0.89 eV. In accord with previous computational studies on helicenes,[4] modifying the geometry and adjusting overlap values to account for the distortion of the rings had very little effect on the results.

The results did, however, improve dramatically when transannular effects were included. Because of the helical geometry, atoms at one end of the molecule find themselves in close proximity to atoms at the other (Figure 4). Overlap integrals were therefore assigned to pairs of proximate atoms. For instance, the carbonyls on the inside of helix **1** should overlap even though they are at opposite ends of the molecule. The distance in neutral **1** between the carbonyl carbon at one end and the carbonyl oxygen at the other is known from the X-ray diffraction analysis to be 2.85 Å.[13] Note that while the overlap around the helix occurs in the usual π-sense, the transannular overlap between the carbonyls occurs in a pseudo-Möbius sense, the top of the carbon lobe overlapping with the bottom of the oxygen lobe at the other end of the molecule. The sign of this overlap integral was therefore inverted. Values for the overlap integrals were those used by Koutecky and Paldus[7] in their calculation of the electronic structure of the benzene π-dimer. The distances between the overlapping atoms were in the case of $\mathbf{2}^-$ those shown by the crystal structure of the neutral bisquinone, in the case of $\mathbf{1}^-$ and $\mathbf{3}^-$ those calculated by ab initio methods,[14] and in the case of $\mathbf{4}^-$ those estimated by extrapolation from the other structures.

We have previously shown that the near-IR transitions of quinone anion radicals can be calculated as the difference in energy between the two lowest unoccupied molecular orbitals of the neutral molecule,[11] which we term SOMO and LUMO for the radical anion. Using this approach, the values of the transition energies in the near-IR for the helical anion radicals were calculated with reasonable accuracy (Table II). The absolute transition energies are underestimated by an average of 0.26 eV (similar errors were found for linear quinone anion radicals), and the relative transition energies in the series $\mathbf{1}^-$–$\mathbf{6}^-$ are assessed accurately.

An especially interesting result is that the transannular interaction between the inner carbonyls of $\mathbf{1}^-$ is bonding. That is, there is no node between the proximate atoms in the SOMO. Geometry-optimized ab initio calculations, to be reported elsewhere, have confirmed this result.[14] They show that the transannular C–O distance for neutral **1** should be 2.78 Å, in good agreement with the distance found in the crystal structure (2.85) Å. The same interatomic distance in the radical anion was calculated ab initio to be 2.51 Å.[14] This implies that bonding between the rings

(9) Manning, W. B.; Kelly, T. P.; Muschik, G. M. *J. Org. Chem.* **1980**, *45*, 2535.
(10) Rosen, B. I.; Weber, W. P. *J. Org. Chem.* **1977**, *42*, 3463.
(11) (a) Powers, M. J.; Meyer, T. J. *J. Am. Chem. Soc.* **1978**, *100*, 4393. (b) Tom, G. M.; Creutz, C.; Taube, H. *J. Am. Chem. Soc.* **1974**, *96*, 7827. (c) Hush, N. S. *Prog. Inorg. Chem.* **1967**, *8*, 391. (d) Wong, K. Y.; Schatz, P. N. *Prog. Inorg. Chem.* **1981**, *28*, 369.
(12) Liberko, C. A.; Rak, S. F.; Miller, L. L. *J. Org. Chem.* **1992**, *57*, 1379.
(13) We thank Prof. Gerard Parkin for this analysis.
(14) Unpublished work of J. E. Almlöf and A. Sargent.

Table III. ESR Proton Hyperfine Splitting

proton	^aH (exp), G	^aH (calc), G	proton	^aH (exp), G	^aH (calc), G
1a	0.73	0.60	4b	1.20	1.10
1b	2.00	1.80	4c		0.02
1c,e	0.16	0.00, 0.00	4d	0.55	0.85
1d	0.55	0.44	4e,f,g,h		0.46, 0.17, 0.01, 0.38
2a	0.60	0.89	5a	0.95	0.73
2b	1.20	1.06	5b	1.75	1.75
2c		0.00	5c,d		0.02, 0.07
2d	1.30	1.22	6a	1.60	1.17
2e	0.15	0.53	6b	1.18	1.10
2f		0.09	6c,d		0.13, 0.02
3a	0.90	0.99	7a	2.50	2.41
3b	1.50	1.42	7b	2.70	2.47
3d	0.86	0.75	7c		0.06
3c,e,f,g	0.26	0.01, 0.07, 0.01, 0.08	7d	1.10	1.36
4a	1.18	0.98	7e,f,g,h		0.42, 0.40, 0.23, 0.51

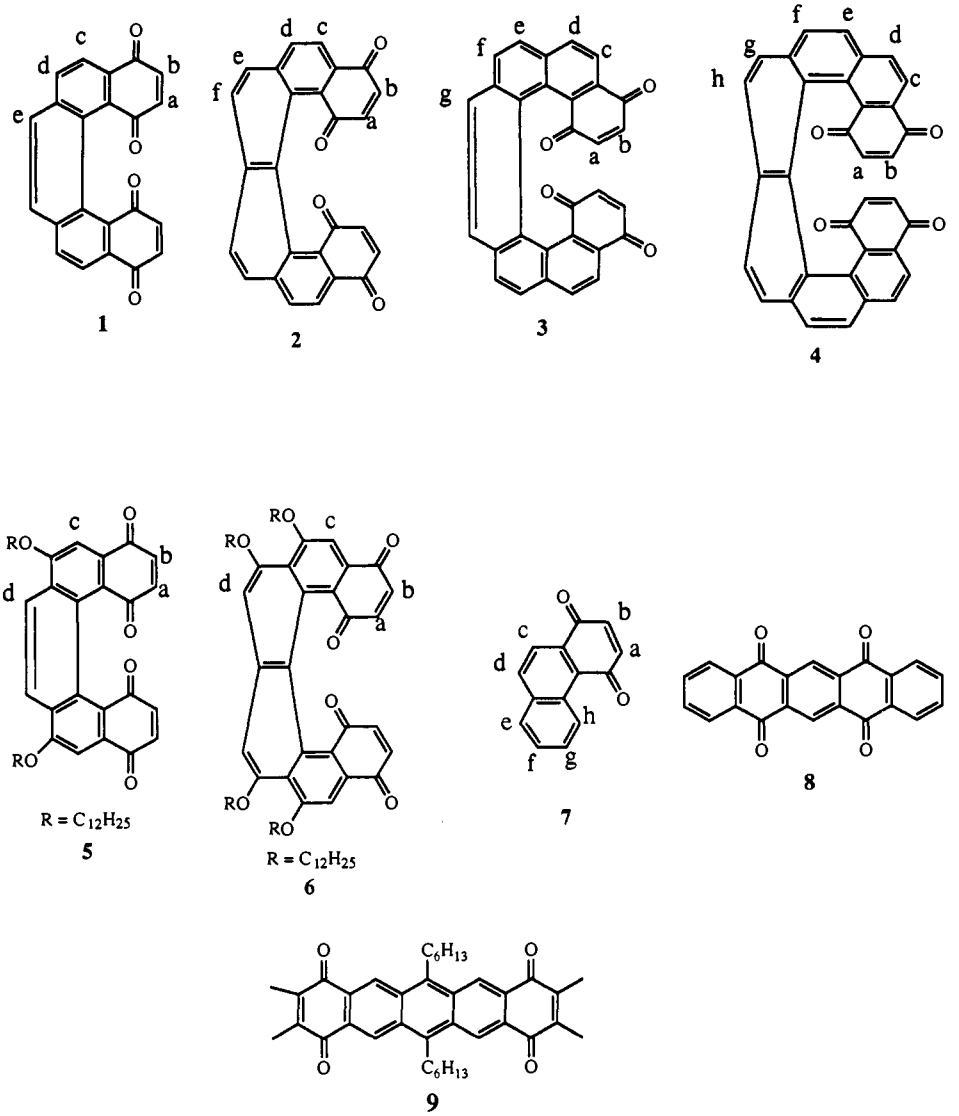

Figure 1. Structure of quinones 1–9.

at opposite ends of the molecule is significant. Thus unlike in neutral helical hydrocarbons,[4] in the quinone anion-radicals the odd electron delocalizes not only around the helical π-system but also transannularly, bonding the ends of the anion radical.

ESR

The electrochemically generated radical anions all display resolved ESR spectra. The spectra were simulated mathematically, and the hyperfine splittings are listed in Table III. The assignment of specific a_H values to specific protons (identified by letter in Figure 1) was made using electron densities from those PPP calculations that gave the near-IR transitions quoted in Table II. The McConnell[15] equation with q = 27 G was used to convert electron densities to a_H values. Note that all the hyperfine splittings occur in pairs, indicating that the unpaired electron interacts equally with the protons on both sides of the molecule. The spectrum of the monoquinone 7^-, of course, showed splittings

(15) McConnell, H. M. *J. Chem. Phys.* **1956**, *24*, 764. McConnell, H. M.; Chesnut, D. B. *J. Chem. Phys.* **1958**, *28*, 107.

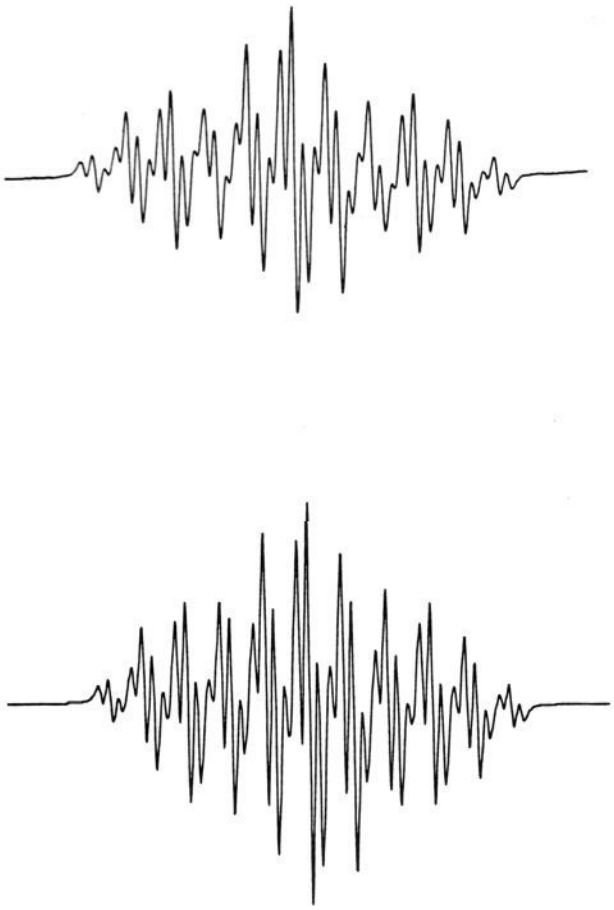

Figure 2. ESR spectrum of $\mathbf{1}^-$ in DMF solution (0.1 M n-Bu_4N^+ BF_4^-). Observed (top) and simulated (bottom). Spectral width is 10 G.

by single protons.

The spectrum and simulation for $\mathbf{1}^-$ are shown in Figure 2. The 39 line pattern did not change when the temperature was varied from 220–360 K, indicating that the odd electron is either delocalized or hops rapidly on the time-scale of the experiment (10^{-8} s). At about 220 K the intensity decreased, and below 210 K, when the solvent froze, it was completely lost. The signal reappeared when the sample was rewarmed above 220 K. Heating the sample above 360 K caused it to decompose. The temperature independent splittings are consistent with our hypothesis that the odd electron is delocalized over the entire molecule.

The splittings indicate that in $\mathbf{1}^-$ the electron density is highest on the quinone groups (a_H = 2.00 and 0.73 G, two protons each) but is also significant on the helicene rings, where the couplings to the attached protons are 0.55 and 0.16 G. When the proton at position 1d is replaced by an alkoxy group (compound $\mathbf{5}^-$), the 39 line pattern is replaced by one that is much simpler, with only seven lines. The two largest splittings are slightly changed (to 1.75 and 0.95 G), while the splitting assigned to the proton at the substituted position disappears. This supports the assignments and shows that there is significant electron density on the bridging non-quinone rings, as expected for a delocalized anion radical.

The spectrum and simulation for $\mathbf{3}^-$ are shown in Figure 3. The 25 line pattern from the four pairs of protons, assigned by PPP calculations, also shows that while the electron density is greatest in the quinone groups (a_H = 1.50 and 0.90 G), considerable electron density is located on the other rings (a_H = 0.86 and 0.26 G).

Anion $\mathbf{2}^-$ shows an 11 line spectrum, which was simulated assuming splittings by three pairs of protons with a_H = 1.30, 1.20, and 0.60 G. In this case the calculation assigns the largest splitting to a pair of protons on the helicene bridging unit. Tetraalkoxy substitution as in $\mathbf{6}^-$ simplifies the pattern to nine lines. This pattern is that expected if there are two pair of protons with a_H = 1.60 and 1.18 G. Both the experimental and calculated values show that the tetraalkoxy substitution greatly increases the electron density in the quinone unit.

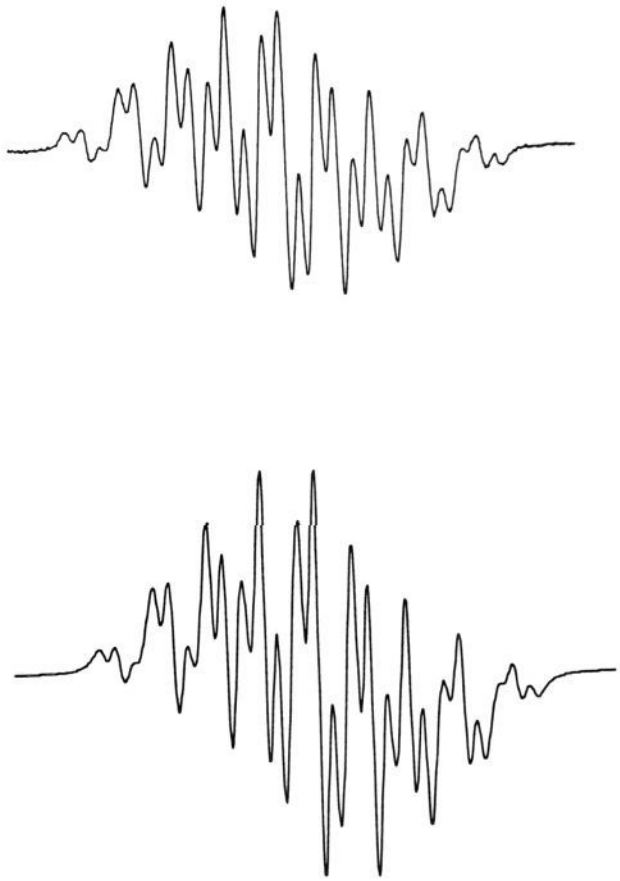

Figure 3. ESR spectrum of $\mathbf{3}^-$ in DMF solution (0.1 M n-Bu_4N^+ BF_4^-). Observed (top) and simulated (bottom). Spectral width is 10 G.

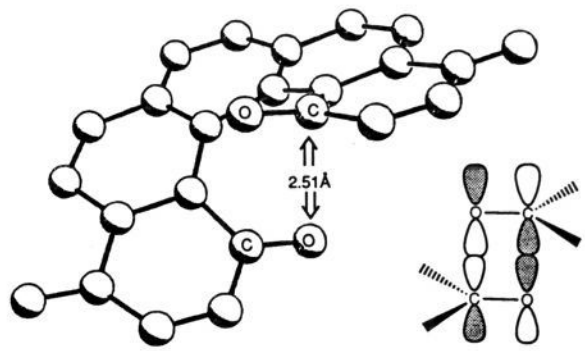

Figure 4. Geometry of $\mathbf{1}^-$ as calculated ab initio showing the proximity of the carbonyls on the inner helix of the molecule. The bonding overlap in the SOMO is shown (inset).

Although PPP calculations, which assumed delocalization around the helix and across the transannular gap, gave satisfactory agreement for each of the anion radical ESR spectra, these calculations have a certain ad hoc quality to them. Calculations performed without the inclusion of transannular overlap were also performed for $\mathbf{1}^-$–$\mathbf{6}^-$. In the case of $\mathbf{1}^-$ and $\mathbf{5}^-$ these calculations did not give satisfactory agreement with experiment.

A second question of interest regards localization. Since the ESR spectra of $\mathbf{1}^-$ and $\mathbf{2}^-$ were independent of temperature down to 220 K, the barrier to hopping between two localized structures would have to be less than 4 kcal mol^{-1}. Furthermore, the relatively large coupling constants for the non-quinone bridge hydrogens implies that the electron density is not localized on the quinone moieties. Even so, ESR cannot absolutely rule out

localization. In this regard anion radical $\mathbf{2}^-$ is of special interest, because the spectrum expected from a localized electronic structure with rapid hopping can be simulated using parameters measured for $\mathbf{7}^-$. The spectrum of $\mathbf{7}^-$ consists of the six-line pattern expected if the splitting is by three individual protons with a_H = 2.50, 2.70, and 1.10 G. Rapid hopping of the electron between two phenanthraquinone fragments of $\mathbf{2}^-$ would then be expected to give a spectrum with twice as many splittings each with half the value (three pairs of protons a_H = 1.25, 1.35, and 0.55 G). These values are close to those observed, reinforcing the concern that ESR cannot distinguish delocalized structures from localized ones if there is a small barrier to electron hopping.

Conclusions

Reduction potentials and the near-IR and ESR spectra of $\mathbf{1}$–$\mathbf{6}^-$ are consistent with the hypothesis that these anion radicals, unlike the linear analog, $\mathbf{9}^-$, are delocalized. This delocalization is not only around the helix but also across the gap between the ends of the molecule. The evidence is particularly compelling for the five-ringed radical anion $\mathbf{1}^-$, which exhibits a large separation in reduction potentials, a calculable electronic transition energy, a fairly intense and solvent independent near-IR band, and a calculable temperature independent ESR spectrum with high electron density on the non-quinone bridge hydrogens. For the larger helicene–bisquinones, all the data are consistent with delocalization, and the near-IR spectra strongly support helically delocalized structures. Such structures are unique and impart unusual physical properties, the most remarkable of which are the π^*–π^* bands occurring at wavelengths from 1.4 to 2.2 μm.

Acknowledgment. This work was supported by the National Science Foundation. The ESR simulation program was supplied by P. Kasai. We thank J. Almlöf for discussions and the ab initio calculations.

Probing Ergot Alkaloid Biosynthesis: Intermediates in the Formation of Ring C

Alan P. Kozikowski,[†] Chinpiao Chen,[†] Jiang-Ping Wu,[‡] Masaaki Shibuya,[§] Chun-Gyu Kim,[⊥] and Heinz G. Floss*,[⊥]

Contribution from the Mayo Clinic Jacksonville, Jacksonville, Florida 32224, and Departments of Chemistry, University of Pittsburgh, Pittsburgh, Pennsylvania 15260, The Ohio State University, Columbus, Ohio 43210, and University of Washington, Seattle, Washington 98195.
Received October 28, 1992

Abstract: The mode of C-ring formation in ergot alkaloid biosynthesis was probed by synthesizing two potential intermediates, compounds **6** and **7**, in deuterated form from the prenylated indole **8**. Both compounds were incorporated into the ergot alkaloid elymoclavine by washed mycelia of *Claviceps* sp., strain SD 58, but only the formation of **7**, and not **6**, could be demonstrated in the cultures. Hence it is proposed that only **7** is an intermediate in ergot alkaloid biosynthesis, whereas **6** is not on the pathway but can be converted into **7** when added to the cultures. A pathway is proposed for the formation of ring C involving epoxidation of **7** at the terminal double bond and cyclization of the epoxide with simultaneous decarboxylation.

The biosynthesis of the clinically important ergot alkaloids both in the ergot fungus[1,2] and in higher plants[3] proceeds from the building blocks L-tryptophan, L-methionine, and an isoprene unit derived from mevalonic acid. Much has been learned from tracer studies in fermentations with *Claviceps* species about the assembly of the tetracyclic ergoline ring system from these basic building blocks.[1,2] From these studies the pathway shown in Scheme I has emerged for the formation of elymoclavine (**1**), the precursor of the commercially important lysergic acid derivatives. However, one notable gap in our understanding of this pathway concerns the mode of closure of ring C, i.e., the formation of the tricyclic intermediate, chanoclavine-I (**2**), from its last established precursor,[4] *N*-methyl-4-(γ,γ-dimethylallyl)tryptophan (*N*-methyl-DMAT, **3**).

The formation of **2** proceeds stereospecifically with retention of the original hydrogen from the chiral center of L-tryptophan as H-5[5] and of the *pro-R* hydrogen from C-10 of DMAT as H-10[6] in the final product, **1**. It must involve a cis–trans isomerization at the allylic double bond, since an isotopic label from C-2 of mevalonate, which labels the *E*-methyl group of γ,γ-dimethylallyl pyrophosphate (DMAPP),[7] appears in the methyl and not the hydroxymethyl group of 2,[8] whereas DMAT labeled in the *Z*-methyl group labels exclusively the hydroxymethyl group of **2**.[9] The oxygen atom of the hydroxymethyl group originates from molecular oxygen[10] and must be introduced prior to ring closure, since deoxychanoclavine-I was not incorporated into agroclavine or **1**.[11] Both *E*- and *Z*-4-(4-hydroxy-3-methyl-2-butenyl)tryptophan were incorporated into **1**,[12,13] but a detailed analysis of

* Address reprint requests to this author at Department of Chemistry BG-10, University of Washington, Seattle, WA 98195.
† Mayo Clinic.
‡ University of Pittsburgh.
§ The Ohio State University.
⊥ University of Washington.

(1) Floss, H. G. *Tetrahedron* **1976**, *32*, 873.
(2) Floss, H. G.; Anderson, J. A. In *The Biosynthesis of Mycotoxins—A Study in Secondary Metabolism*; Steyn, P. S., Ed.; Academic Press: New York, 1980; pp 17–67.
(3) Gröger, D.; Mothes, K.; Floss, H. G.; Weygand, F. *Z. Naturforsch.* **1963**, *18B*, 1123.
(4) Otsuka, H.; Quigley, F. R.; Gröger, D.; Anderson, J. A.; Floss, H. G. *Planta Med.* **1980**, *40*, 109 and references therein.
(5) Floss, H. G.; Mothes, U.; Günther, H. *Z. Naturforsch.* **1964**, *19B*, 784.
(6) Shibuya, M.; Chou, H.-M.; Fountoulakis, M.; Hassam, S.; Kim, S.-U.; Kobayashi, K.; Otsuka, H.; Rogalska, E.; Cassady, J. M.; Floss, H. G. *J. Am. Chem. Soc.* **1990**, *112*, 297 and references therein.
(7) Popjak, G.; Cornforth, J. W. *Biochem. J.* **1966**, *101*, 553.
(8) Fehr, T.; Acklin, W.; Arigoni, D. *J. Chem. Soc., Chem. Commun.* **1966**, 801.
(9) Pachlatko, P.; Tabacik, C.; Acklin, W.; Arigoni, D. *Chimia* **1975**, *29*, 526.
(10) Kobayashi, M.; Floss, H. G. *J. Org. Chem.* **1987**, *52*, 4350.
(11) Fehr, T. Ph.D. Dissertation No. 3967, Eidgenössische Technische Hochschule, Zürich, 1967. Arigoni, D. *Symposium on Organic Chemical Approaches to Biosynthesis*; London, 1965.
(12) Plieninger, H.; Wagner, C.; Immel, H. *Liebigs Ann. Chem.* **1971**, *743*, 95.

0002-7863/93/1515-2482$04.00/0